Chiral Mo−Binol Complexes: Activity, Synthesis, and Structure. Efficient Enantioselective Six-Membered Ring Synthesis through Catalytic Metathesis

S. Sherry Zhu,[†] Dustin R. Cefalo,[‡] Daniel S. La,[‡] Jennifer Y. Jamieson,[†] William M. Davis,[†] Amir H. Hoveyda,*[,‡] and Richard R. Schrock*[,†]

Contribution from the Department of Chemistry, Massachusetts Institute of Technology, Cambridge, Massachusetts 02139, and Department of Chemistry, Merkert Chemistry Center, Boston College, Chestnut Hill, Massachusetts 02467

Received May 3, 1999

Abstract: A new class of chiral Mo-based complexes **2a** and **2b**, bearing functionalized chiral binol ligands, is disclosed. Mo complex **2a** promotes the asymmetric ring-closing metathesis (ARCM) of various dienes and trienes to afford six-membered carbo- and heterocycles efficiently and in high optical purity. The binol-based chiral Mo catalysts complement the previously reported biphen-based complexes, which are particularly effective in the enantioselective synthesis of five-membered rings by ARCM. Studies regarding catalytic kinetic resolutions and asymmetric desymmetrizations are described. It is possible to obtain optically pure products in high yield from catalytic reactions without the use of solvent (cf. eq 1). The structural attributes of these complexes are detailed on the basis of the data available from an X-ray structure and variable-temperature ^{1}H NMR studies. The results of this investigation indicate the following: (i) The anti-Mo·THF complex exists as a mixture of diastereomers, whereas the syn isomer is formed stereoselectively. (ii) The anti-Mo isomers are likely more Lewis acidic.

Introduction

Structural modularity is one of the most desirable properties of a catalyst.[1] This attribute facilitates access to various sterically and electronically[2] modified systems and provides the chemist with an opportunity to prepare and screen other potential candidates. Such considerations are important, since subtle structural variations within a substrate often render a previously potent catalyst ineffective.[3]

The chiral Mo-based catalysts **1a**,**b**, which we reported recently, benefit from structural modularity.[4] These complexes can be used to initiate asymmetric ring-closing metathesis (ARCM) of 1,6-dienes to afford five-membered carbo- and heterocycles in high optical purity. However, **1a**,**b** are significantly less effective in promoting the formation of the analogous unsaturated pyrans and cyclohexenes (lower yields and/or selectivities). To address this shortcoming, we turned our attention to the preparation of related catalysts that efficiently promote the enantioselective synthesis of other cyclic structures. Herein, we report that Mo-based complexes **2a** and **2b**, bearing a chiral binol (vs biphen) ligand, deliver chiral cyclohexenes, dihydropyrans, and 1,7-dienes in high optical purity through catalytic resolution and desymmetrization processes.[5]

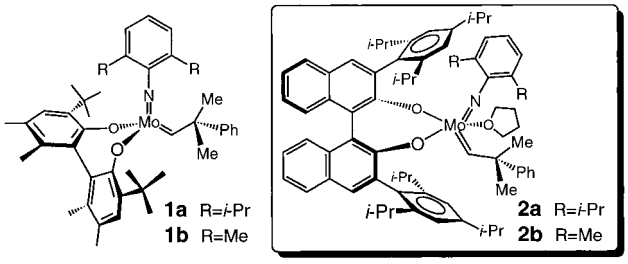

Results and Discussion

1. Chiral Mo−Binaphtholates in Asymmetric Synthesis. a. Catalytic Kinetic Resolution of Dienes. As depicted in Scheme 1, we initially examined the ability of complexes **2a** and **2b** to catalyze the enantioselective formation of five-membered rings by the ARCM of 1,6-dienes. The representative example in Scheme 1 (**3** → **4**) illustrates that, whereas biphen complex **1a** promotes ring closure with high enantiodifferentiation, **2a** does so with significantly reduced selectivity and

[†] Massachusetts Institute of Technology.

[‡] Boston College.

(1) (a) Hoveyda, A. H. *Chem. Biol.* **1998**, *5*, R187−R191. (b) Shimizu, K. D.; Snapper, M. L.; Hoveyda, A. H. *Chem. Eur. J.* **1998**, *4*, 1885−1889.

(2) For selected examples of electronic tuning of transition metal-catalyzed reactions, see: (a) Jacobsen, E. N.; Zhang, W.; Guler, M. L. *J. Am. Chem. Soc.* **1991**, *113*, 6703−6704. (b) Rajanbabu, T. V.; Ayers, T. A.; Casalnuovo, A. L. *J. Am. Chem. Soc.* **1994**, *116*, 4101−4102. (c) Schnyder, A.; Hintermann, L.; Togni, A. *Angew. Chem., Int. Ed. Engl.* **1995**, *34*, 931−933 and references therein.

(3) For a recent example, where structurally related substrates have different optimum chiral catalysts, see: Shimizu, K. D.; Cole, B. M.; Krueger, C. A.; Kuntz, K. W.; Snapper, M. L.; Hoveyda, A. H. *Angew. Chem., Int. Ed. Engl.* **1997**, *36*, 1704−1707.

(4) (a) Alexander, J. B.; La, D. S.; Cefalo, D. R.; Hoveyda, A. H.; Schrock, R. R. *J. Am. Chem. Soc.* **1998**, *120*, 4041−4042. (b) La, D. S.; Alexander, J. B.; Cefalo, D. R.; Graf, D. D.; Hoveyda, A. H.; Schrock, R. R. *J. Am. Chem. Soc.* **1998**, *120*, 9720−9721.

(5) Related Mo complexes have been used in catalyzing ROMP processes: (a) Totland, K. M.; Boyd, T. J.; Lavoie, G. G.; Davis, W. M.; Schrock, R. R. *Macromolecules* **1996**, *29*, 6114−6125. (b) McConville, D. H.; Wolf, J. R.; Schrock, R. R. *J. Am. Chem. Soc.* **1993**, *115*, 4413−4414. (c) O'Dell, R.; McConville, D. H.; Hofmeister, G. E.; Schrock, R. R. *J. Am. Chem. Soc.* **1994**, *116*, 3414−3423.

10.1021/ja991432g CCC: $18.00
Published on Web 08/24/1999

Scheme 1

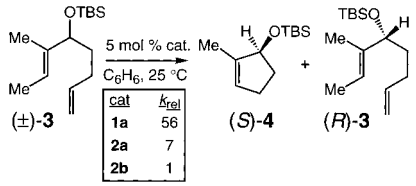

Table 1. Catalytic Enantioselective Carbocycle Synthesis by ARCM[a]

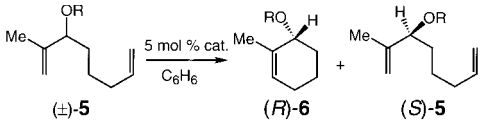

entry	substrate	catalyst	*T* (°C); reaction time	conv[b] (%); dimer (%)	k_{rel}[c,d]
1		**2a**	22; 4 h	66; 34	17
2	(±)-**5a**	**2a**	***65; 40 min***	***77; 27***	***24***
3	R = TES	**2b**	22; 1h	68; 11	4.3
4		**1a**	22; 30 min	58; 11	4.0
5		**2a**	22; 3 h	68; 37	>25
6	(±)-**5b**	**2a**	***65; 35 min***	***65; 23***	***>25***
7	R = TBS	**2b**	22; 1 h	59; 23	2.5
8		**1a**	22; 20 min	82; 7	3.3

[a] Conditions: 5 mol % catalyst, Ar atm, C_6H_6. [b] Conversion determined by analysis of 400 MHz ^{1}H NMR of the unpurified mixture. [c] Enantioselectivity determined by GLC analysis (CHIRALDEX-GTA by Alltech) in comparison with authentic racemic material. [d] Relative rate determined based on the formation and selectivity of product (exclusive of dimer amount).

2b effects RCM without any discrimination between the two diene enantiomers.

As shown in Table 1, *in contrast to biphen Mo complexes, binol Mo systems catalyze the ARCM of 1,7-dienes with excellent enantioselectivity*.[6] In the presence of 5 mol % **2a**, *rac*-**5a** is resolved with excellent efficiency, where k_{rel} = 17 and 24, for reactions at 22 and 65 °C, respectively (entries 1−2, Table 1).[7] Although ARCM catalyzed by biphen-Mo complex **1a** generates lower amounts of dimeric products[8] (11% with **1a** vs >27% with **2a**), these reactions proceed with significantly lower levels of enantiodifferentiation (entry 4, k_{rel} = 4.0). Similar results, as observed for **1a**, are obtained with the sterically less demanding **2b** (entry 3). Additional data in entries 5−8 demonstrate that the binol-based complex **2a** is generally a superior catalyst for the ARCM of 1,7-dienes.

The Mo-catalyzed kinetic resolutions presented in Table 2 provide an even starker contrast between the selectivity patterns observed in ARCM reactions promoted by binol- and biphen-Mo catalysts. *rac*-**7** (entry 1, Table 2) is resolved efficiently within 40 min with 5 mol % **2a** (k_{rel} > 25) with <5% dimeric product formed. Catalytic ARCM promoted by biphen complex **1a** affords a substantial amount of dimer and negligible enantiodiscrimination (entry 2, Table 2). With **1b** as the catalyst, resolution efficiency is higher than that observed with **1a** but still substantially lower than that obtained with **2a**. Similar observations were made with silyl ether **9** as the substrate (entries 4−6, Table 2). It is noteworthy that in resolutions depicted in Table 2 there is generally less dimer formation than in reactions depicted in Table 1. This difference may be attributed to the presence of the sterically bulky dimethylsilyl unit in the former, inhibiting association of two substrate molecules with the chiral transition-metal center.

Table 2. Catalytic Enantioselective Heterocycle Synthesis by ARCM[a]

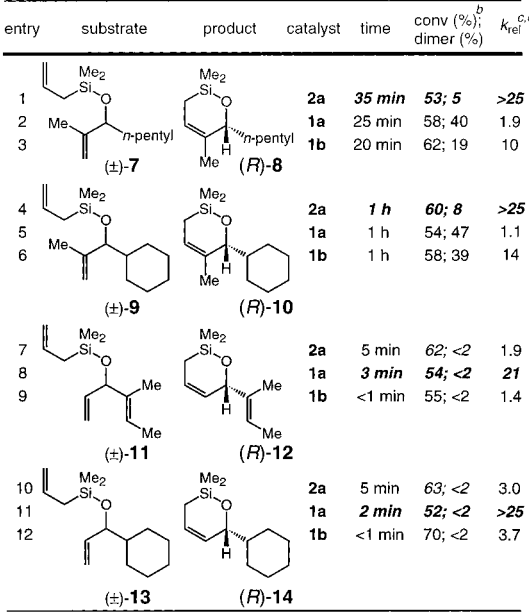

[a−c] See Table 1. [d] Relative rates are based on recovered substrates.

Remarkably, the identity of the optimum catalyst is reversed in the catalytic resolutions of **11** and **13**, where both reactive sites are *terminal* olefins (entries 7−9 and 10−12, Table 2). *With two terminal alkenes as reaction partners, it is the biphen-Mo **1a** that is the superior catalyst* (k_{rel} = 21 and >25 for **11** and **13**, respectively). In both instances, Mo−binaphtholate **2a** and the Mo−biphenolate derivative **1b**, bearing a di*methyl*imido ligand, are hardly stereodifferentiating (k_{rel} <2, entries 7, 9, and k_{rel} <4, entries 10, 12, Table 2). Furthermore, ARCM of **11** underlines the high levels of regiocontrol involved with the formation of initial Mo-alkylidene and subsequent RCM; there is <2% product derived from the reaction of the trisubstituted olefin. It is difficult to offer at the present time a rational hypothesis as to why **2a** is the superior catalyst for reactions that involve the more substituted alkenes (**7** and **9**), whereas **1a** is the preferred catalyst when two terminal alkenes are involved (**11** and **13**). These results, however, highlight the advantages inherent in the structural modularity of the present class of Mo catalysts. In addition, these data caution us against overgeneralizing the selectivity profiles of various chiral Mo-based metathesis catalysts.

b. Catalytic Asymmetric Desymmetrization of Trienes. The ARCM processes presented in Table 3 involve the catalytic desymmetrization of 1,6- and 1,7-dienes. As depicted in entry 1 (Table 3), **2a** is unable to initiate RCM. In this case, it is **2b** that effectively initiates the ARCM of **15**. Consistent with the

(6) Attempts at Mo-catalyzed ARCM of 1,7-dienes related to **3** at 22 °C (where one alkene is trisubstituted) resulted in exclusive dimer formation (by reaction of terminal alkenes).

(7) The k_{rel} values are calculated by the equation reported by Kagan. See: Kagan, H. B.; Fiaud, J. C. *Top. Stereochem.* **1988**, *18*, 249−330. This calculation is only an approximation of the relative rates of reactions of the two enantiomers, as it is based on a first-order equation, where a simultaneous process (dimerization) does not occur (see footnote 8 for dimer definition).

(8) By dimeric product we mean the material obtained by catalytic intermolecular cross-coupling of two substrate molecules through their terminal alkenes. The dimeric adduct (mixture of olefin isomers) from diene **5a**, shown below, is illustrative.

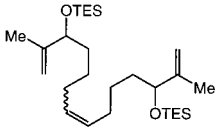

Table 3. Enantioselective Synthesis of Six-Membered Ring Heterocycle by Mo-Catalyzed Desymmetrization[a]

entry	substrate	product	catalyst	time (h); temp (°C)	conv (%);[c] dimer (%)	yield (%);[d] ee (%)[b]
1	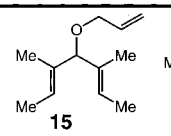	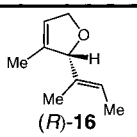	**2a**	18; 22	<5; --	--; --
2			**2b**	18; 22	80; <2	77; 89
3	**15**	(*R*)-**16**	**1b**	***6: 22***	***93; <2***	***83; 99***
4	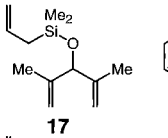	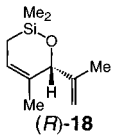	**2a**	***3; 60***	***>99; <2***	***98; >99***
5			**1a**	24; 22	50; 32	17; 65
6	**17**	(*R*)-**18**	**1b**	24; 22	51; 28	20; 85
7[e]	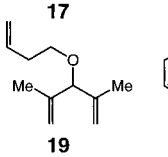	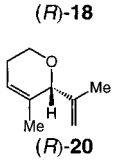	**2a**	***3; 60***	***95; <2***	***86; >99***
8			**1a**	3; 22	72; 6	--; 96
9	**19**	(*R*)-**20**	**1b**	3; 22	65; 38	--; 86

[a−c] See Table 1. [d] Isolated yields after silica gel chromatography. [e] Reactions in entries 7−9 were performed in *n*-pentane due to high product volatility.

aforementioned selectivity trends, the biphen complex **1b** proves to be the best choice for the asymmetric formation of the *five*-membered ring (*R*)-**16**.

In contrast, **2a** readily promotes the conversion of silyl ether **17** to the *six*-membered ring allyl silane (*R*)-**18**; this transformation occurs within 3 h in >99% ee (chiral GLC) and 98% isolated yield after silica gel chromatography. Biphen-based catalysts **1a** and **1b** are significantly less effective: after 24 h, there is ∼50% conversion, **18** is formed with substantially lower levels of enantioselection, and the major product is the derived dimer. It is particularly noteworthy that, although biphen complexes **1a** and **1b** afford substantial amounts of dimer in the presence of **17**, *with **2a** as catalyst (eq 1), even in the absence of solvent, <2% dimer is obtained;* ARCM product (*R*)-**18** is isolated in 98% yield and >99% ee after distillation.

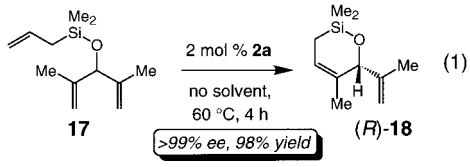

Similar, but less pronounced, trends are observed in the Mo-catalyzed desymmetrizations of triene **19**. Once again, the Mo−binaphtholate **2a** affords optically pure (*R*)-**20** efficiently and in excellent yield (86% after silica gel chromatography).

2. Synthesis of Mo−Binaphthol Complexes. Binaphthol **23** was prepared as depicted in Scheme 2 (sequence shown is for the *R* isomer). The ligand synthesis utilizes dimethyl ether **21**, which is available from double-alkylation of commercially available, optically pure binaphthol.[9] Subsequent directed double-deprotonation,[10] followed by bromination of the resulting dianion, delivers dibromide **22**. Ni-catalyzed cross-coupling[10] with 2,4,6-tri(isopropyl)phenylmagnesium bromide[11] and deprotection of the resulting methyl ethers affords **23** (42% overall yield; $[\alpha]^{22}_D = 88.0$ ($c = 3.0$, THF)). Optically pure **2a** and **2b** are then prepared in analogy to the previously reported syntheses of **1a** and **1b**.[4] Both complexes are recrystallized as THF adducts (from Et_2O at −35 °C in the presence of THF).

Scheme 2[a]

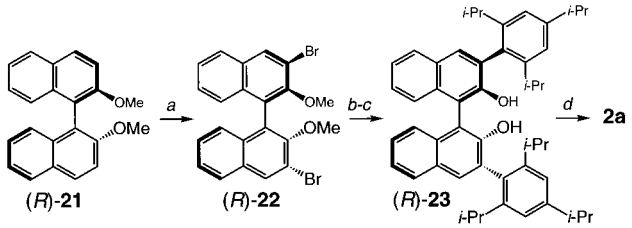

[a] Key: (a) TMEDA, *n*-BuLi, Et_2O, 22 °C, 4 h; Br_2, Et_2O, −40 → +22 °C, 8 h (71% overall); (b) 1.0 mol % $(PPh_3)_2NiCl_2$, 2,4,6-tri(isopropyl)phenylmagnesium bromide, Et_2O, 45 °C, 24 h, 70%; (c) BBr_3, CH_2Cl_2, 22 °C, 12 h, 83%; (d) benzylpotassium, THF, 10 min; $Mo(CHCMe_2Ph)(NAr)(OTf)_2$·dme, THF, 22 °C, 15 min, 64% (Ar = 2,6-diisopropylPh).

3. Structure of Mo−Binaphthol Complexes. a. X-ray Crystallography. Mo complexes **2a** and **2b** are obtained as yellow crystals that contain 1 equiv of THF. On the basis of ^{1}H NMR studies (detailed below) and the previously reported X-ray structure of the analogous *anti*-**24** (shown in Scheme 3),[5a] it is likely that THF is a ligand in the Mo complex.

Crystals of pyridine adduct **25** (bearing (*R*)-**23**) were found to be suitable for X-ray crystallography (Scheme 3; selected numbering and *i*-Pr groups omitted for clarity). In this structure, pyridine is coordinated to one of the two diastereotopic CNO faces of the Mo complex (complexes shown in Scheme 3 represent coordination from the two CNO faces).[12] The resulting trigonal bipyramid, with the alkylidene and imido ligands positioned equatorially, is similar to the structures of related Mo or W complexes.[13]

Several structural features of *syn*-**25** merit additional discussion. The Mo−C(1) (Mo=C_α) bond distance (1.840(12) Å) and Mo=C_α-C_β bond angle (149.5(10)°) are typical of the syn isomers of this class of transition metal complexes (Table 4).[4,5]

Table 4. Selected Bond Distances (Å) and Angles (deg) in Mo Complexes 24 and 25

complex *anti*-**24**		complex *syn*-**25**	
Mo−N(1)	1.732(7)	Mo−N(1)	1.715(10)
Mo−C(33) (Mo−C_α)	1.927(9)	Mo−C(1) (Mo−C_α)	1.840(12)
Mo−O(1)	1.988(5)	Mo−O(1)	1.988(7)
Mo−O(2)	2.012(5)	Mo−O(2)	2.018(7)
Mo−O(3)	2.195(5)	Mo−N(2)	2.251(10)
Mo−N(1)−C(101)	166.9(6)	Mo−N(1)−C(11)	158.6(8)
Mo−O(2)−C(17)	112.8(5)	Mo−O(2)−C(101)	122.3(6)
C(33)−Mo−O(1)	127.4(3)	C(1)−Mo−O(1)	117.8(4)
C(33)−Mo−O(2)	92.5(3)	C(1)−Mo−O(2)	86.1(4)
N(1)−Mo−C(33)	100.3(3)	N(1)−Mo−C(1)	110.8(5)
N(1)−Mo−O(1)	131.3(3)	N(1)−Mo−O(1)	130.6(4)
N(1)−Mo−O(2)	100.4(3)	N(1)−Mo−O(2)	105.8(3)
O(1)−Mo−O(2)	87.8(2)	O(1)−Mo−O(2)	86.5(3)
O(1)−Mo−O(2)	78.4(2)	O(1)−Mo−N(2)	78.5(3)
N(1)−Mo−O(3)	88.8(3)	N(1)−Mo−N(2)	87.9(4)
O(2)−Mo−O(3)	166.2(2)	O(2)−Mo−N(2)	164.2(3)
C(33)−Mo−O(3)	96.1(3)	C(1)−Mo−N(2)	96.5(4)
C(1)−C(2)−C(22)−C(17)	65.5[a]	C(201)−C(202)−C(102)−C(101)	60.0[a]

[a] The dihedral angle between the two naphthyl rings in the binaphtholate ligands.

Overall, the structure of *syn*-**25** (Table 1) is comparable to that of the closely related *anti*-**24** (Scheme 4). It is, however, important to note two structural variations between these two metal systems. (i) Mo complex *anti*-**24** contains a smaller Mo=

(9) Both antipodes of binaphthol are commercially available (Aldrich Co. and Kankyo Kagaku Center Co., Japan).

(10) (a) Lingenfelter, D. S.; Helgeson, R. C.; Cram, D. J. *J. Org. Chem.* **1981**, *46*, 393−406. (b) Hu, Q. S.; Vitharana, D.; Ou, L. *Tetrahedron: Asymmetry* **1995**, *6*, 2123−2126.

(11) 1-Bromo-2,4,6-triisopropylbenzene is commercially available (Alfa/Aesar).

(12) Wu, Y.-D.; Peng, Z.-H. *J. Am. Chem. Soc.* **1997**, *119*, 8043−8049.

(13) Feldman, J.; Schrock, R. R. *Prog. Inorg. Chem.* **1991**, *39*, 1−74.

Scheme 3

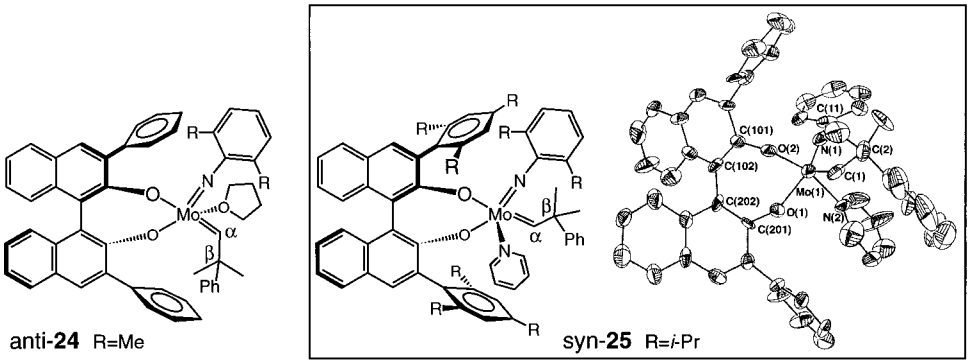

$C_\alpha-C_\beta$ bond angle (128.1(6)°) than *syn*-**25** (149.5 (10)°). (ii) *anti*-**24** has a longer Mo−C(33) bond (1.927(9) Å) than *syn*-**25** (1.840 (12) Å). These differences can be rationalized in the following manner:

(a) $Mo{=}C_\alpha-C_\beta$ bond angles in syn complexes (e.g., **25**) are larger than those in anti isomers, due (in part) to the steric interaction between the alkylidene unit pointing toward the ortho substituents of the phenylimido ligand (Scheme 4).

Scheme 4[a]

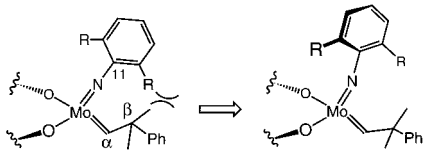

[a] The steric interaction shown above causes the following: (i) larger $N-Mo-C_\alpha$ angle; (ii) bending of $Mo-N-C_{11}$ bond; (iii) twisting of the imido ligand.

In *syn*-**25**, steric interaction between the alkylidene unit and the imido ligand *o*-*i*-Pr substituent (Scheme 4) causes the Mo−N−C(11) bond system to bend from its preferred linear orientation (158.6 (8)° and 166.9 (6)° in *syn*-**25** and *anti*-**24**, respectively).[14] Such interactions cause the twisting of the 2,6-diisopropylphenyl ring. The 2,6-$Me_2C_6H_3$ ring in *anti*-**24** can lie in the $N-Mo-C_\alpha-C_\beta$ plane because of the lesser steric interaction between the imido and alkylidene groups.

(b) As illustrated in Figure 1, and as supported by various theoretical studies,[15] an agostic interaction[16] between the $H-C_\alpha$ bond and the transition metal might be partially responsible for

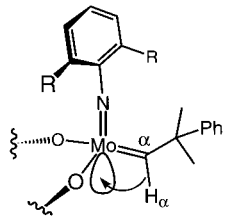

Figure 1. Agostic interaction between alkylidene CH and σ^* Mo−N leads to shortening of the Mo=C bond.

the shorter $Mo{=}C_\alpha$ bond of the syn isomer. Thus, hyperconjugation ($\sigma_{C-H} \rightarrow \sigma^*_{Mo-N}$) increases the p character of the $H-C_\alpha$ and the s character of the $Mo{=}C_\alpha$ bond, giving the latter partial triple bond character.

b. NMR Studies. A ^{13}C NMR spectrum (22 °C) of **25** shows an alkylidene peak (Mo=C) at 309 ppm that we ascribe to the more abundant syn adduct.[5,17] The ^1H NMR spectrum of **25** (Figure 2, 20 °C, C_6D_6) exhibits one sharp resonance at 13.110 ppm and two (∼1:1) signals at 14.290 and 14.371 ppm in a ratio of 88:12 (syn peak: both anti peaks). A high-intensity ^1H NMR spectrum reveals ^{13}C satellites on the alkylidene resonances. The high-field H_α resonance (Mo=CH) exhibits $J_{C\alpha H\alpha} = 114$ Hz and is assigned to the syn isomer.[16b] The two lower field H_α resonances are attributed to anti alkylidenes, based on the larger coupling constant ($J_{C\alpha H\alpha} = 147$ Hz). Two anti isomers likely arise from coordination of pyridine to the two CNO faces of the Mo complex (see below for further discussion).

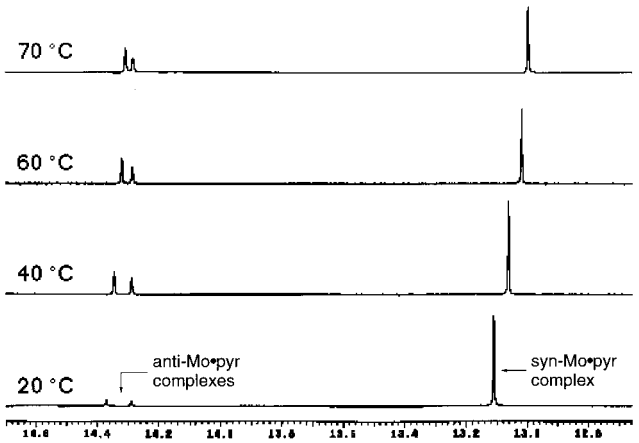

Figure 2. Alkylidene region (Mo=C*H*) from variable-temperature ^1H NNR experiments with **7**.

The chemical shifts of signals corresponding to both the syn and anti H_α nuclei appear to be somewhat temperature-dependent. The resonance corresponding to the syn isomer shifts upfield upon heating. When the sample is heated to 70 °C, the ratio of the H_α resonances for the anti adduct relative to those for the syn adduct becomes 43:57 (from 12:88). It is plausible that the syn/anti ratio changes as a consequence of pyridine dissociation, followed by equilibration by rotation about the

(14) The bending caused by steric strain is reinforced by lowering of the overlap between the imido N nonbonding electrons into a Mo d orbital, reducing the triple bond character of the Mo−N bond. Thus, the Mo−N bond regains some of its double bond character to cause the observed change in bond angles. For a review on orbital ineractions involved in the syn−anti isomerization of this class of Mo complexes, see: Schrock, R. R. In *Alkene Metathesis in Organic Synthesis*; Furstner, A., Ed.; Springer: Berlin 1998; pp 1−37.

(15) (a) Reference 12. (b) Folga, E.; Ziegler, T. *Organometallics* **1993**, *12*, 325. (c) Monteyne, K.; Ziegler, T. *Organometallics* **1998**, *17*, 5901−5907. (d) Cundari, T. R.; Gordon, M. S. *Organometallics* **1992**, *11*, 55−63. (e) Fox, H. H.; Schofield, M. H.; Schrock, R. R. *Organometallics* **1994**, *13*, 2804−2815.

(16) (a) Schrock, R. R. In *Reactions of Coordinated Ligands*; Braterman, P. R., Ed.; Plenum: New York, 1986; pp 221−283. (b) Brookhart, M.; Green, M. L. H.; Wong, L. *Prog. Inorg. Chem.* **1988**, *36*, 1−124.

(17) Schrock, R. R.; Crowe, W. E.; Bazan, G. C.; DiMare, M.; O'Regan, M. B.; Schofield, M. H. *Organometallics* **1991**, *10*, 1832−1843.

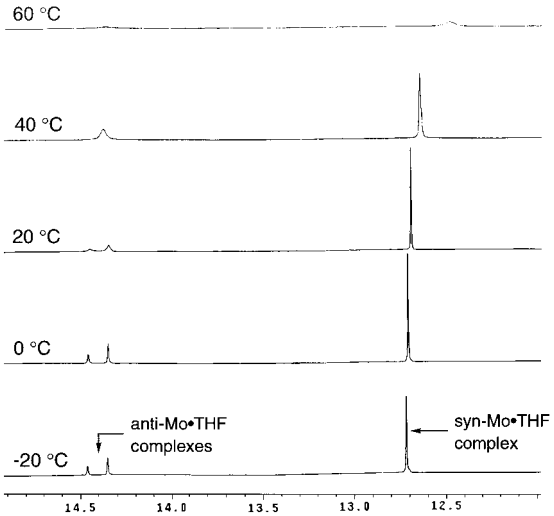

Figure 3. Alkylidene region (Mo=C*H*) from the variable-temperature ^{1}H NMR experiments with **2a** (excess THF, toluene-d_8).

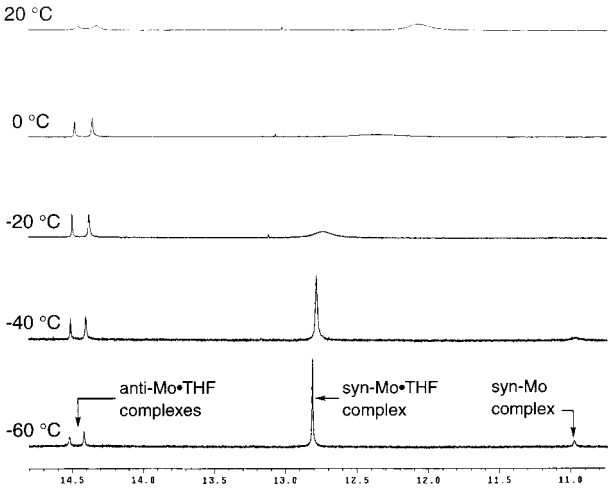

Figure 4. Alkylidene region (Mo=C*H*) from the variable-temperature ^{1}H NMR experiments involving **2a** from which THF has been partially removed.

Mo=C$_\alpha$ bond.[18] It must be noted that *two* resonances for *each* alkylidene isomer would have been observed if pyridine were to bind indiscriminately to the two diastereotopic CNO faces in each isomer. Several explanations may be put forth as to why only one syn H$_\alpha$ resonance is observed:[19] (i) pyridine binds to only one CNO face of the syn isomer; (ii) both syn diastereomers are present in solution, but the H$_\alpha$ resonances happen to have the same chemical shift; and (iii) pyridine rapidly dissociates from and reassociates with the complex, allowing two diastereomeric syn complexes to equilibrate rapidly on the NMR time scale without the base free complex being observed. It is not likely that there is rapid equilibration between **25** and the corresponding base-free complex, a pathway that is probably required for interconversion of the derived diastereomers.[20] This contention is supported by the following observations: (i) The ^{1}H NMR resonances are sharp. (ii) Heating of the NMR sample to 70 °C and subsequent recooling does not result in regeneration of the *initial* syn/anti isomer ratios observed at 22 °C (pyridine does not readily dissociate at ambient temperature).

The related ^{1}H NMR spectra of **2a** (500 MHz, toluene-d_8) are more complex than those of **25**; this can be ascribed to the higher lability (lower Lewis basicity) of THF. Accordingly, for the sake of simplicity, we decided to examine the spectra derived from samples of **2a** in the presence of excess THF, so as to minimize the presence of any THF-free Mo complex. As shown in Figure 3, the ^{1}H NMR spectrum of **2a** (−20 °C) in the presence of excess THF reveals two anti alkylidene H$_\alpha$ signals and one syn alkylidene H$_\alpha$ resonance. As the temperature is raised, the H$_\alpha$ signals for the two diastereomeric anti THF adducts (14.5−14.3 ppm) broaden and coalesce at ∼33 °C. The broadening and coalescence of the two anti H$_\alpha$ resonances may be ascribed to the rapid interconversion of the two anti THF diastereomers.

As illustrated in Figure 3, the signal from the syn isomer begins to shift upfield when the sample temperature is above 40 °C. As mentioned before in connection to the pyridine-bound complex **25**, this is likely the result of THF dissociation to afford the free syn complex, with which the syn THF adduct exchanges rapidly. In contrast there is little change in the average chemical shift of the anti isomer upon heating. *These observations imply that the anti isomer is more Lewis acidic than the syn isomer*, since the latter more readily loses its THF ligand (additional supporting data is provided below).[20] This hypothesis is consistent with, inter alia, the suggested agostic interaction in this class of syn Mo complexes (cf. electron donation from C−H to Mo in Figure 1).

A sample of **2a**, from which THF is *partially* removed by subjection of the sample to vacuum, was examined by ^{1}H NMR spectroscopy. Partial removal of THF was effected so as to allow the detection of the THF-bound as well as any derived THF-free Mo complex (temperature range is different than that used in Figure 2). Indeed, as illustrated in Figure 4, at −60 °C, the ^{1}H NMR spectrum of **2a** exhibits an H$_\alpha$ resonance at 10.98 ppm for the THF-free syn isomer and one for the THF-bound syn adduct (12.810 ppm). In addition, there are two signals for the diastereotopic anti-THF complexes (14.520 and 14.416 ppm); however, there are no signals corresponding to the THF-free *anti*-**2a**. *The spectrum obtained at −60 °C therefore suggests that the THF complex derived from the syn isomer is formed diastereoselectively*.[21]

As the sample temperature is raised (−40 °C → 20 °C, Figure 4), the H$_\alpha$ signal for the THF-free *syn*-**2a** broadens and coalesces with that for the THF-bound syn adduct, an observation that again points to the higher lability of a THF ligand in the corresponding syn complex compared to the more Lewis acidic anti isomer. In accord with the proposal that the anti isomer is more Lewis acidic, the rate and degree of THF dissociation at 20 °C is sufficiently small that it does not lead to a significant variation in the chemical shift of the H$_\alpha$ resonances of *anti*-**2a** (∼14.5−14.4 ppm) or rapid interconversion of diastereomers.

The above data imply that the average resonance for the interconverting *syn*-THF adduct and its parent base-free complex can be used to estimate the concentration of these entities in solution. These measurements are based on the assumption that the Mo−alkylidene H$_\alpha$ resonances for the THF-bound and free complex are not significantly temperature dependent (compared to the chemical shift difference between the THF-bound and THF-free syn complex, cf. Figure 4). Accordingly, based on

(18) Alexander, J. B.; Hoveyda, A. H.; Schrock, R. R. Unpublished results. The assumption that pyridine (or THF) dissociation is required before syn: anti isomerization occurs, is supported by previous studies on the effect of added PMe$_3$ on the syn and anti forms of Mo(NAr)(CHCMe$_2$Ph)[OCMe(CF$_3$)$_2$]$_2$; see ref 17.

(19) These mechanistic possibilities are based on the theoretically supported assumption that an approaching Lewis base binds to the metal complex through one of the CNO faces (see ref 17).

(20) Oskam, J. H.; Schrock, R. R. *J. Am. Chem. Soc.* **1993**, *115*, 11831−11845.

(21) The identity of the major syn THF-bound diastereomer has not yet been determined.

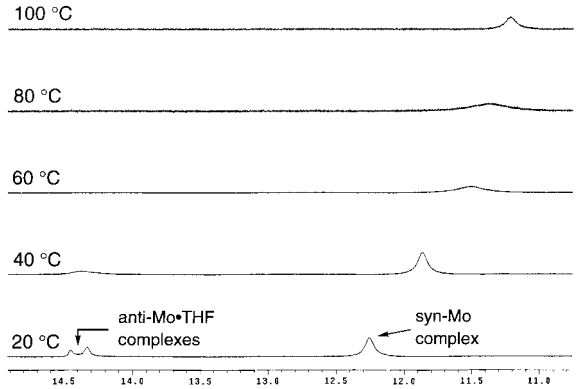

Figure 5. Alkylidene region (Mo=C*H*) from the variable-temperature ^{1}H NMR experiments involving **2a** (toluene-d_8).

the average resonance for the THF-bound and THF-free syn complex, $K_{eq} \cong 2$ at 20 °C for the *syn*-THF complex and its corresponding THF-free isomer.

With the above information in hand, we turned our attention to variable-temperature ^{1}H NMR experiments with a sample of Mo complex **2a** (no excess THF added nor any removed). As illustrated in Figure 5, the significant shift of the syn Mo=CH signal (20 → 40 °C, Figure 5) is due to the rapid loss of THF from the syn isomer and a rapid equilibrium between the THF-bound and free complexes (cf. Figure 5). At 40 °C, the signal for the alkylidene CH of the THF-bound and more Lewis acidic anti complex begins to broaden and shift, as it too begins to lose its THF ligand.[22]

On the basis of studies with analogous THF-free biphenoxide complexes,[18] it is likely that further broadening of both syn and anti alkylidene H_α signals between 60 and 80 °C arises from interconversion of THF-free *syn*-**2a** and *anti*-**2a**. Thus, as depicted in Figure 5, when the sample is heated to 100 °C, the sharpening signal likely represents the average of all possible THF-free and THF-bound complexes. Moreover, consistent with the relative Lewis acidity of *syn*- vs *anti*-**2a**, while *syn*-**2a** releases a THF ligand readily at 40 °C, *anti*-**2a** is relatively resistant to the loss of THF. It is nonetheless important to note the following: (i) There are as yet no direct data concerning the relative reactivity of the syn and anti isomers of binol-based chiral Mo complex **2a**. The relative reactivity of syn and anti isomers may vary among different Mo complexes (from variations in imido, diolate, and alkylidene ligands). (ii) The relative reactivity of syn and anti isomers may further depend on the electronic and steric nature of the approaching olefin.[17]

Conclusions

We disclose a class of chiral Mo-based catalysts that effect the enantioselective formation of a range of six-membered carbo- and heterocycles. Catalysts **2a**,**b** are complementary to the previously reported biphen-based systems;[4] they significantly enhance the synthetic utility of catalytic metathesis in asymmetric synthesis. Although binol complexes are typically more effective in the asymmetric synthesis of six-membered rings by ARCM, one cannot always predict which class of catalysts is the best choice. Catalytic ARCM of a 1,6-diene is likely most efficiently promoted by a Mo−biphen complex and that of a 1,7-diene by a Mo−binol catalyst, but subtle substrate structural variations can cause such roles to be reversed (e.g., entries 7−12, Table 2). At the present time it is difficult to provide a plausible rationale for the selectivity trends exhibited by the two classes of catalysts (complexes **1** vs **2**); future mechanistic and modeling work will hopefully lead to the formulation of an effective model. Nonetheless, the findings detailed here offer a compelling case for the continued development of chiral metathesis catalysts.[23]

Several structural features of these complexes emerge through examination of X-ray data and various NMR studies. Noteworthy is the apparent higher Lewis acidity of the anti Mo isomers and the diastereoselective coordination of THF to the syn, but not anti, complex.

The synthesis and development of additional classes of chiral Mo catalysts and investigation of their ability to promote ARCM and other metathesis-based processes are in progress. The results of these studies will be revealed shortly.

Experimental Section

General Information. Infrared (IR) spectra were recorded on Perkin-Elmer 781 and 1608 spectrophotometers, ν_{max} in cm^{-1}. Bands are characterized as broad (br), strong (s), medium (m), and weak (w). ^{1}H NMR spectra were recorded on Varian GN-400 (400 MHz), Unity 300 (300 MHz), and Varian VXR 500 (500 MHz) spectrometers. Chemical shifts are reported in ppm from tetramethylsilane with the solvent resonance as the internal standard ($CHCl_3$: δ 7.26). Data are reported as follows: chemical shift, multiplicity (s = singlet, d = doublet, t = triplet, q = quartet, br = broad, m = multiplet), coupling constants (Hz), integration, and assignment. ^{13}C NMR spectra were recorded on a Varian GN-400 (100 MHz), Unity 300 (75 MHz), and Varian VXR 500 (125 MHz) spectrometers with complete proton decoupling. Chemical shifts are reported in ppm from tetramethylsilane with the solvent as the internal reference ($CDCl_3$: δ 77.7 ppm). Conversions were determined by ^{1}H NMR of the unpurified reaction mixtures. Enantiomer ratios were determined by chiral GLC analysis (Alltech Associates Chiraldex GTA column (30m × 0.25 mm)) or Betadex 120 column (30m × 0.25 mm) in comparison with authentic materials. Microanalyses were performed by Robertson Microlit Laboratories (Madison, NJ) and Microlytics Analytical Laboratories (Deerfield, MA). High-resolution mass spectrometry was performed by the University of Illinois and Massachusetts Institute of Technology Mass Spectrometry Laboratories.

All reactions were conducted in oven (135 °C) and flame-dried glassware under an inert atmosphere of dry argon. Benzene, toluene, and *n*-pentane were distilled from sodium metal/benzophenone ketyl. *n*-Pentane was stirred over concentrated H_2SO_4 for 5 days and then distilled over Na. Mo(N-2,6-*i*-$Pr_2C_6H_3$)(CHCMe$_2$Ph)(OTf)$_2$·DME and Mo(N-2,6-$Me_2C_6H_3$)(CHCMe$_2$Ph)(OTf)$_2$·DME were synthesized according to a published procedure.[24] Mo(N-2,6-^{i}Pr$_2$C$_6$H$_3$)(CHCMe$_2$Ph)((*S*)-(−)-*t*-Bu$_2$Me$_4$(biphen))[4b] and Mo(N-2,6-Me$_2$C$_6$H$_3$)(CHCMe$_2$Ph)((*S*)-(−)-*t*-Bu$_2$Me$_4$(biphen))[4b] were synthesized on the basis of previously reported procedures.

(*R*)-(+)-Mo(*N*-2,6-*i*-$Pr_2C_6H_3$)(CHCMe$_2$Ph)(3,3′-bis(2,4,6-triisopropylphenyl)-2,2′-dihydroxy-1,1′-dinaphthyl)(THF) (2a). To a stirred solution of (*R*)-3,3′-bis(2,4,6-triisopropylphenyl)-2,2′-dihydroxy-1,1′-dinaphthyl (**23**) (3.4 g in 250 mL of THF, 4.9 mmol) was added benzylpotassium (1.34 g, 10.3 mmol) slowly at 22 °C. The resulting solution turned from colorless to yellow over the course of 10 min. At this point, Mo(*N*-2,6-*i*-$Pr_2C_6H_3$)(CHCMe$_2$Ph)(OTf)$_2$·DME (3.5 g, 4.4 mmol) was added in a single portion. After the mixture was allowed to stir at 22 °C for 15 min, volatile solvents were removed in vacuo from the resulting red solution to yield a dark red solid. This residue was washed with 20 mL of benzene and filtered through Celite. Removal of solvents in vacuo afforded a red solid, which was washed with cold Et_2O (5 mL) and again filtered through Celite. The Et_2O solution was cooled to −35 °C to afford 2.0 g (36% yield) of **2a** as a yellow solid. ^{1}H NMR (300 MHz, toluene-d_8): δ 14.45 (s (br), 23%

(22) The H_α resonance in free anti-**2a** is likely to be upfield of that for THF-bound *anti*-**2a** on the basis of studies involving other complexes in this general family. See ref 5.

(23) For a related study in this area, see: Fujimura, O.; Grubbs, R. H. *J. Am. Chem. Soc.* **1996**, *118*, 2499−2500.

(24) Schrock, R. R.; Murdzek, J. S.; Bazan, G. C.; Robbins, J.; DiMare, M.; O'Regan, M. *J. Am. Chem. Soc.* **1990**, *112*, 3875−3886.

of 1H, anti-C*H*CMe$_2$Ph), 14.30 (s (br), 24% of 1H, anti-C*H*CMe$_2$Ph), 12.26 (s (br), 53% of 1H, syn-C*H*CMe$_2$Ph), 7.75 (s, 2H, Ar*H*), 7.65−7.60 (m, 4H, Ar*H*), 7.18−6.90 (s (br), Ar*H*), 6.81 (s, 4H, Me$_2$CHC$_6$*H*$_2$), 3.26 (s (br), THF), 3.08 (s (br), THF), 3.96−2.72 (s (br), 8H, Me$_2$C*H*), 1.48 (s, 3H, CHC(C*H*$_3$)$_2$Ph), 1.45 (s, 3H, CHC(C*H*$_3$)$_2$Ph), 1.28−0.71 (s (br), CH(C*H*$_3$)$_2$ and THF), 0.70 (d, J = 6.0 Hz, 14H, (C*H*$_3$)$_2$CH). ^{13}C NMR (125 MHz, toluene-d_8): δ 321.8, 154.7, 150.7, 148.6, 148.2, 147.8, 147.2, 137.6, 137.2, 136.6, 136.1, 132.4, 132.0, 130.3, 130.2, 129.6, 128.9, 128.6, 127.9, 127.4, 126.9, 126.6, 126.5, 126.2, 125.8, 124.1, 123.6, 121.4, 121.2, 120.9, 73.1, 66.3, 54.5, 35.4, 35.1, 32.4, 31.7, 31.5, 30.4, 29.4, 28.7, 27.2, 26.6, 25.7, 25.3, 25.1, 24.9, 24.7, 24.6, 24.2, 23.4, 21.3, 21.1, 20.5, 20.4, 16.0, 2.4. Anal. Calcd for $C_{76}H_{93}NO_3Mo$: C, 78.39; H, 8.05; N, 1.20. Found: C, 78.46; H, 8.12; N, 1.24.

(*R*)-(+)-Mo(*N*-2,6-Me$_2$C$_6$H$_3$)(CHCMe$_2$Ph)(3,3′-bis(2,4,6-triisopropylphenyl)-2,2′-dihydroxy-1,1′-dinaphthyl)(THF) (2b). Complex **2b** was synthesized according to the above procedures, except that Mo(*N*-2,6-Me$_2$C$_6$H$_3$)(CHCMe$_2$Ph)(OTf)$_2$·DME was used as the starting material. ^{1}H NMR (300 MHz, CDCl$_3$): δ 14.24 (s, 27% of 1H, C*H*CMe$_2$Ph), 11.90 (s (br), 73% of 1H, C*H*CMe$_2$Ph), 7.82 (s, 1H, Ar*H*), 7.74−6.59 (m, 19H, Ar*H*), 6.54 (s, 2H, Ar*H*), 3.50−2.78 (m, 9H, THF, (CH$_3$)$_2$C*H*), 2.40 (s, 1H, (CH$_3$)$_2$C*H*), 1.83−1.53 (s (br), 3H, Mo=CH-(C*H*$_3$)), 1.37−0.61 (m, 49 H, Mo=CH(C*H*$_3$), CH(C*H*$_3$)$_2$, Ar(C*H*$_3$)$_2$, THF). ^{13}C NMR (125 MHz, C$_6$D$_6$): δ 287.3, 156.7, 151.6, 150.5, 149.9, 149.4, 148.8, 148.0, 147.6, 136.3, 135.3, 134.7, 134.2, 133.6, 132.7, 131.4, 130.7, 130.1, 128.9, 127.6, 126.9, 126.5, 125.5, 125.1, 124.6, 123.8, 123.4, 114.4, 75.3, 72.0, 66.3, 54.8, 53.1, 36.0, 35.6, 35.0, 32.6, 31.6, 31.2, 29.5, 29.1, 26.9, 26.4, 25.7, 24.6, 23.1, 19.6, 15.9, 14.6. Anal. Calcd for $C_{72}H_{85}NO_3Mo$: C, 78.02; H, 7.73; N, 1.26. Found: C, 77.88; H, 7.84; N, 1.32.

Representative Procedure for Mo-Catalyzed Kinetic Resolution (at 22 °C). 2-Methyl-3-*tert*-butyldimethylsiloxy-1,7-octadiene (**5b**) (0.15 g, 0.59 mmol) was dissolved in benzene (5.9 mL) in a capped vial (to allow for the release of ethylene). Optically pure catalyst (**2a**) (0.034 g, 0.029 mmol, 5 mol %) was then added. The resulting mixture was allowed to stir at 22 °C for ∼3.5 h. At this point, the reaction mixture was exposed to air; subsequently, methanol (1 mL) was added. Removal of the volatiles in vacuo afforded a dark red oil. Percent conversion was calculated by analysis of the ^{1}H NMR spectrum (500 MHz, CDCl$_3$). The starting material, metathesis product, and dimeric products were isolated by silica gel chromatography (hexanes). In the case of highly volatile products, percent conversion was determined by the analysis of the ^{1}H NMR spectrum of the unpurified reaction mixture (C$_6$D$_6$).

Representative Procedure for Mo-Catalyzed Kinetic Resolution (Temperatures above 22 °C). 2-Methyl-3-*tert*-butyldimethylsiloxy-1,7-octadiene (**5b**) (0.15 g, 0.59 mmol) was dissolved in benzene (5.9 mL) in a tightly capped vial (to prevent solvent loss). Optically pure catalyst (**2a**) (0.034 g, 0.029 mmol, 5 mol %) was added to this solution as a solid. The resulting orange solution was placed into a heated bath (equilibrated to 60 °C) for ∼35 min. At this time, the reaction mixture was exposed to air and methanol (1 mL) was added. In analogy to the purification procedure mentioned above, the percent conversion was determined, and starting material, metathesis product, and dimeric product were isolated. In the case of highly volatile products, percent conversion was determined by analysis of the ^{1}H NMR of the unpurified reaction mixture (C$_6$D$_6$).

(*R*)-2-Methyl-1-triethylsiloxy-2-cyclohexene (6a). IR (NaCl): 2962 (s), 2873 (s), 1457 (m), 1243 (m), 1086 (m), 1004 (s) cm^{-1}. ^{1}H NMR (400 MHz, CDCl$_3$): δ 5.50 (s, 1H, CH$_2$C*H*=C), 4.04 (s (br), 1H, C*H*OSi), 2.01 (d, J = 18.4 Hz, 1H, C*H*HCH=C), 1.88 (d, J = 18.4 Hz, 1H, C*H*HCH=C) 1.78−1.47 (m, 4H, C*H*$_2$CH$_2$), 1.71 (s, 3H, CH=CC*H*$_3$), 0.98 (t, J = 8.0 Hz, 9H, (C*H*$_3$CH$_2$)$_3$SiO), 0.64 (q, J = 8.0 Hz, 6H, (CH$_3$C*H*$_2$)$_3$SiO). ^{13}C NMR (100 MHz, CDCl$_3$): δ 136.6, 125.5, 69.9, 33.7, 26.2, 21.5, 19.6, 7.6, 5.7. Anal. Calcd for $C_{13}H_{26}OSi$: C, 68.96; H, 11.57. Found: C, 68.76; H, 11.43.

(*R*)-2-Methyl-1-*tert*-butyldimethylsiloxy-2-cyclohexene (6b). IR (NaCl): 2929 (w), 2857 (s), 1603 (w), 1462 (m), 1375 (m), 1250 (s), 1073 (m), 1038 (s), 1019 (s), 1004 (s) cm^{-1}. ^{1}H NMR (300 MHz, CDCl$_3$): δ 5.48 (s, 1H, CH$_2$C*H*=CCH$_3$), 4.03 (s, 1H, C*H*OSi), 2.05−1.80 (m, 2H, C*H*$_2$CH=CCH$_3$), 1.78−1.59 (m, 2H, C*H*$_2$CH$_2$CHC=C), 1.68 (s (br), 3H, CH=CC*H*$_3$), 1.53−1.46 (m, 2H, C*H*$_2$CHOSi), 0.90 (s (br), 9H, (C*H*$_3$)$_3$CSi), 0.09 (s, 6H, C*H*$_3$SiC*H*$_3$). ^{13}C NMR (75 MHz, CDCl$_3$): δ 124.7, 114.2, 69.7, 33.2, 26.2, 25.7, 21.2, 19.3, −4.1, −4.5. Anal. Calcd for $C_{13}H_{26}OSi$: C, 68.96; H, 11.57. Found: C, 68.71; H, 11.39.

(*R*)-1-Oxa-6-pentyl-2-sila-2,2,5-trimethyl-cyclohex-4-ene (8). IR (NaCl): 2962 (s), 2936 (s), 2867 (m), 1457 (m), 1376 (w), 1262 (s), 1224 (w), 1105 (m) cm^{-1}. ^{1}H NMR (400 MHz, CDCl$_3$): δ 5.61−5.57 (m, 1H, C=C*H*), 4.21 (s (br), 1H, OC*H*), 1.61 (s, 3H, C*H*$_3$C=CH), 1.59−1.13 (m, 10H, C*H*$_2$C*H*$_2$C*H*$_2$C*H*$_2$CH$_3$, SiC*H*$_2$CH), 0.88 (t, J = 6.8 Hz, 3H, CH$_2$CH$_2$CH$_2$C*H*$_3$), 0.17 (s, 3H, SiC*H*$_3$), 0.09 (s, 3H, SiC*H*$_3$). ^{13}C NMR (100 MHz, CDCl$_3$): δ 139.0, 120.0, 77.1, 36.7, 32.6, 25.3, 23.4, 22.8, 14.8, 13.0, 1.5, 0.2. HRMS (EI$^+$): calcd for $C_{12}H_{24}OSi$ 212.1596, found 212.1603. Anal. Calcd for $C_{12}H_{24}OSi$: C, 67.86; H, 11.39. Found: C, 67.90; H, 11.15.

Determination of the Stereochemical Identity of Mo-Catalyzed Kinetic Resolution Products. A sample of optically enriched (*R*)-**7** was prepared through silylation of a sample of optically enriched allylic alcohol, prepared by the method of Sharpless.[25] The product obtained from the Mo-catalyzed ARCM was correlated with this authentic material.

(*R*)-1-Oxa-6-cyclohexyl-2-sila-2,2,5-trimethyl-cyclohex-4-ene (10). IR (NaCl): 2930 (s), 2861 (m), 1464 (w), 1256 (m), 1111 (m) cm^{-1}. ^{1}H NMR (400 MHz, CDCl$_3$): δ 5.64 (d, J = 8.4 Hz, 1H, SiCH$_2$C*H*), 4.04 (s, 1H, SiOC*H*), 1.77−1.72 (m, 2H, Cy-*H*), 1.63−1.34 (m, 9H, C*H*$_3$C=CH, Cy-*H*), 1.28−1.02 (m, 5H, SiC*H*$_2$CH, Cy-*H*), 0.17 (s, 3H, SiC*H*$_3$), 0.07 (s, 3H, SiC*H*$_3$). ^{13}C NMR (100 MHz, CDCl$_3$): δ 137.9, 120.6, 81.7, 43.5, 31.0, 27.5, 27.2, 27.2, 26.7, 23.3, 13.2, 0.9, 0.2. Anal. Calcd for $C_{13}H_{24}OSi$: C, 69.58; H, 10.78. Found: C, 69.64; H, 10.62.

(*R*)-2,2-Dimethyl-6-(2(*E*)-ethenyl)-1-oxa-2-silacyclohex-4-ene (12). IR (NaCl): 3018 (m), 2968 (m), 2917 (w), 1652 (m), 1564 (m), 1249 (s), 1180 (s), 1080 (m) cm^{-1}. ^{1}H NMR (400 MHz, CDCl$_3$): δ 5.93−5.87 (m, 1H, CH$_3$C*H*=C) 5.53−5.44 (m, 2H, SiCH$_2$C*H*=C*H*), 4.74 (dd, J = 2.4, 2.4 Hz, 1H, OC*H*), 1.61 (d, J = 7.6 Hz, 3H, C*H*$_3$CH), 1.58 (d, J = 1.2 Hz, 3H, C*H*$_3$C) 1.37−1.14 (m, 2H, SiC*H*$_2$CH), 0.19 (s, 3H, SiC*H*$_3$), 0.17 (s, 3H, SiC*H*$_3$). ^{13}C NMR (100 MHz, CDCl$_3$): δ 138.1, 132.2, 125.2, 121.6, 79.4, 13.9, 12.7, 11.7, 0.9, 0.0. HRMS (EI$^+$) calcd for $C_{10}H_{18}OSi$ 182.1127, found 182.1125.

(*R*)-6-Cyclohexyl-2,2-dimethyl-1-oxa-2-silacyclohex-4-ene (14). IR (NaCl): 3018 (w), 2936 (s), 2848 (s), 1646 (w), 1457 (m), 1394 (w), 1256 (s), 1168 (s), 1111 (s) cm^{-1}. ^{1}H NMR (400 MHz, CDCl$_3$): δ 5.90−5.85 (m, 1H, OCHCH=C*H*), 5.57−5.54 (m, 1H, OCHC*H*=CH), 4.18 (dd, J = 2.0, 0.8 Hz, 1H, SiOC*H*), 1.72 (d, J = 9.6 Hz, 2H, SiC*H*$_2$), 1.67−1.62 (m, 2H, Cy-*H*), 1.43−1.37(m, 2H, Cy-*H*), 1.27−0.96 (m, 7H, Cy-*H*), 0.16 (s, 3H, SiC*H*$_3$), 0.13 (s, 3H, SiC*H*$_3$). ^{13}C NMR (100 MHz, CDCl$_3$): δ 131.9, 125.0, 77.3, 45.8, 29.3, 28.5, 27.3, 27.1, 27.0, 13.2, 1.0, 0.0. HRMS (EI$^+$): calcd for $C_{12}H_{22}OSi$ 210.1440, found 210.1440.

(*R*)-2-(2(*E*)-*sec*-Butenyl)-3-methyl-2,5-dihydrofuran (16). IR (NaCl): 2976 (s), 2917 (s), 2845 (s), 1762 (m), 1430 (m), 1380 (m), 1297 (w), 1250 (w), 1184 (w), 1054 (s) cm^{-1}. ^{1}H NMR (500 MHz, CDCl$_3$): δ 5.60 (dq, J = 3.0, 1.0 Hz, 1H, OC*H*(C=C)$_2$), 5.55 (m, 1H, CH$_3$*H*C=CCH$_3$), 5.25−5.19 (m, 1H, OCH$_2$C*H*=C), 4.64 (m, 2H, OC*H*$_2$-CH=C), 1.66 (dq, J = 7.0, 1.0 Hz, 3H, CH$_3$HC=CC*H*$_3$), 1.60 (s (br), 3H, C*H*$_3$HC=CCH$_3$), 1.50 (dq, J = 3.0, 1.0 Hz, 3H, OCH$_2$HC=CC*H*$_3$). ^{13}C NMR (125 MHz, CDCl$_3$): δ 137.3, 135.7, 123.9, 121.6, 95.1, 75.7, 13.6, 12.6, 10.2. HRMS (EI$^+$): calcd for $C_9H_{14}O$ 138.1045, found 138.1045.

(*R*)-1-Oxa-6-(2-propenyl)-2-sila-2,2,5-trimethylcyclohex-4-ene (18). IR (NaCl): 2974 (m), 2924 (m), 2836 (w), 1464 (w), 1275 (s), 1099 (s), 1055 (s) cm^{-1}. ^{1}H NMR (400 MHz, CDCl$_3$): δ 5.72−5.70 (m, 1H, *H*C=CCH$_3$), 4.92 (dd, J = 1.2, 1.2 Hz, 1H, *H*HC=CCH$_3$), 4.85 (t, J = 1.2 Hz, 1H, H*H*C=CCH$_3$), 4.62 (s (br), 1H, OC*H*), 1.66 (t, J = 0.8 Hz, 3H, HC=CC*H*$_3$), 1.55 (dd, J = 1.2, 1.2 Hz, 3H, CH$_2$=CC*H*$_3$), 1.35−1.14 (m, 2H, SiC*H*$_2$CH), 0.19 (s, 3H, SiC*H*$_3$), 0.12 (s, 3H, SiC*H*$_3$). ^{13}C NMR (100 MHz, CDCl$_3$): δ 146.5, 136.0, 121.1, 113.8, 82.1, 22.4, 17.2, 13.0, 0.8, 0.0. HRMS (EI$^+$): calcd for $C_{10}H_{18}OSi$ 182.1127, found

(25) Gao, Y.; Hanson, R. M.; Klunder, J. M.; Ko, S. Y.; Masamune, H.; Sharpless, K. B. *J. Am. Chem. Soc.* **1987**, *109*, 5767−5780 and references therein.

Scheme 5

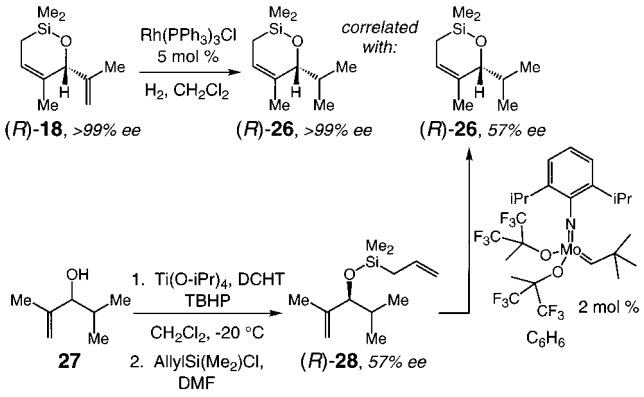

182.1129. Anal. Calcd for $C_{10}H_{18}OSi$: C, 65.87; H, 9.95. Found: C, 65.80; H, 10.00.

Determination of the Stereochemical Identity of Catalytic Desymmetrization Products. As illustrated in Scheme 5, Ti-catalyzed kinetic resolution of allylic alcohol **27**, followed by the installment of the requisite allylsilyl chloride, led to the formation of optically enriched (*R*)-**28**. Subsequent catalytic RCM with 2 mol % (Mo(N-2,6-*i*-$Pr_2C_6H_3$)(CHCMe$_2$Ph)(OCCH$_3$(CF$_3$)$_2$)$_2$)[24] resulted in the formation of an authentic sample of (*R*)-**26**. This material was compared by chiral GLC (BETADEX chiral column) with a sample of optically pure (*R*)-**26**, obtained from the site-selective Rh-catalyzed hydrogenation of (*R*)-**18** (derived from Mo-catalyzed desymmetrization of **17**).

2-*iso*-Propenyl-3-methyl-5,6-dihydro-2*H*-pyran (20). ^{1}H NMR (400 MHz, $CDCl_3$): δ 5.67 (s (br), 1H, C=C*H*CH$_2$), 4.99 (t, J = 1.2 Hz, 1H, C=C*H*H), 4.96 (s, 1H, C=CH*H*), 4.36 (s, 1H, CC*H*O), 3.90 (ddd, J = 10.8, 4.8, 3.2 Hz, 1H, CH$_2$C*H*HO), 3.58 (ddd, J = 12.8, 8.8, 4.0 Hz, 1H, CH$_2$CH*H*O), 2.26−2.17 (m, 1H, CHC*H*HCH$_2$), 1.97−1.92 (m, 1H, CHCH*H*CH$_2$), 1.67 (s (br), 3H, C*H*$_3$C=CH$_2$), 1.51 (d, J = 1.2 Hz, 3H, C*H*$_3$C=CH). ^{13}C NMR (100 MHz, $CDCl_3$): δ 144.5, 134.3, 122.0, 116.1, 82.6, 63.0, 26.2, 20.2, 18.1. HRMS (EI$^+$): calcd for $C_9H_{14}O$ 138.1045, found 138.1045.

(*R*)-3,3′-Dibromo-2,2′-dimethoxy-1,1′-dinaphthyl (22). A solution of *n*-BuLi (28 mL, 2.5 M in hexanes, 70 mmol) and tetramethylethylenediamine (TMEDA; 7.80 g, 67.0 mmol) was added to Et_2O (500 mL) and allowed to stir for 15 min. To this solution was added solid (*R*)-2,2′-dimethoxy-1,1′-dinaphthyl (10.0 g, 31.8 mmol). After 4 h, the brown dilithium salt precipitateed from solution. The reaction mixture was then cooled to −35 °C, and Br_2 (8.0 mL, 65.3 mmol) was added over a period of 0.5 h. The resulting white suspension was allowed to warm to 22 °C and stirred for 2 h. At this point, the mixture was cooled to 0 °C, and 50 mL of water was added. Aqueous extraction with Et_2O (3 × 50 mL) was followed by drying of the organic layers over anhydrous $MgSO_4$ and removal of the volatiles in vacuo. At this point, (*R*)-3,3′-dibromo-2,2′-dimethoxy-1,1′-dinaphthyl (**22**) precipitated from the ether solution as a white solid (9.90 g, 66% yield). The ^{1}H NMR spectrum proved to be identical to that reported in the literature.[10a] $[\alpha]_{589}$ = +71.4 (c = 1.4, THF).

(2,4,6-Triisopropylphenyl)magnesium Bromide. A three-neck round-bottom flask containing Mg (3.00 g, 125 mmol) was equipped with a condenser and an addition funnel. A 10.0 mL portion of a 1.4 M solution of 2,4,6-triisopropylphenyl bromide (20.0 g in 50 mL of Et_2O, 70.6 mmol) was added to the flask through the addition funnel. After 5 min, 0.20 mL (0.002 mmol) of 1,2-dibromoethane was added to the mixture. Once the solution began to reflux, the remaining 2,4,6-triisopropylphenyl bromide solution was slowly added over 1 h. After the addition was complete, the reaction was allowed to reflux for 12 h. The resulting Grignard reagent was then titrated and stored in a drybox.

***rac*- and (*R*)-3,3′-Bis(2,4,6-triisopropylphenyl)-2,2′-dimethoxy-1,1′-dinaphthyl.** (*R*)-3,3′-Dibromo-2,2′-dimethoxy-1,1′-dinaphthyl (4.0 g, 8.5 mmol) and Ni(PPh$_3$)$_2$Cl$_2$ (0.60 g, 11 mol %, 0.90 mmol) were suspended in 100 mL of Et_2O. To this suspension was added (2,4,6-triisopropylphenyl)magnesium bromide (0.8 M, 31.7 mL, 25.4 mmol) slowly at 22 °C. The mixture was allowed to stir at 22 °C for 10 min; at this point, the resulting dark green solution was refluxed for 24 h. The reaction was then allowed to chill to 0 °C and quenched slowly by the addition of 50 mL of a 1.0 M solution of HCl. The resulting aqueous layer was separated from the Et_2O layer and washed three times with excess Et_2O (50 mL). The resulting organic layers were then dried over $MgSO_4$; volatile solvents were removed in vacuo to afford the unpurified residue as a white solid that was then recrystallized from CH_2Cl_2/hexanes to afford (*R*)-3,3′-bis(2,4,6-triisopropylphenyl)-2,2′-dimethoxy-1,1′-dinaphthyl as a white solid (4.7 g, 77% yield). ^{1}H NMR (500 MHz, $CDCl_3$): δ 7.82 (d, J = 8.5 Hz, 2H, Ar*H*), 7.71 (s, 2H, Ar*H*), 7.39 (t, J = 6.0 Hz, 2H, Ar*H*), 7.35−7.31 (m, 4H, Ar*H*), 7.07 (d, J = 9.0 Hz, 4H, Ar*H*), 3.04 (s, 6H, OC*H*$_3$), 2.99−2.93 (m, 2H, C*H*(CH$_3$)$_2$), 2.88−2.85 (m, 2H, C*H*(CH$_3$)$_2$), 2.82−2.76 (m, 2H, C*H*(CH$_3$)$_2$), 1.54 (s, 12H, CH(C*H*$_3$)$_2$), 1.29 (d, J = 7.0 Hz, 6H, CH(C*H*$_3$)$_2$), 1.13 (d, J = 8.0 Hz, 6H, CH(C*H*$_3$)$_2$), 1.09 (d, J = 6.5 Hz, 6H, CH(C*H*$_3$)$_2$), 1.04 (d, J = 6.0 Hz, 6H, CH(C*H*$_3$)$_2$). ^{13}C NMR (125 MHz, $CDCl_3$): δ 155.4, 148.4, 147.3, 147.0, 134.4, 134.2, 133.5, 131.4, 131.2, 130.5, 128.2, 126.2, 126.1, 125.0, 124.8, 120.9, 60.1, 34.6, 31.3, 31.2, 25.8, 25.6, 24.5, 24.4, 23.7, 23.7. HRMS (FAB) calcd for $C_{52}H_{62}O_2$ 718.4750, found (M$^+$) 718.4750. Anal. Calcd for $C_{52}H_{62}O_2$: C, 86.86; H, 8.69. Found: C, 86.62; H, 8.77.

***rac*- and (*R*)-3,3′-Bis(2,4,6-triisopropylphenyl)-2,2′-dihydroxy-1,1′-dinaphthyl (23).** A solution of 3,3′-bis(2,4,6-triisopropylphenyl)-2,2′-dimethoxy-1,1′-dinaphthyl (4.0 g, 5.60 mmol) in 150 mL of CH_2Cl_2 was charged with 39.0 mL of a 1.0 M BBr_3 solution in CH_2Cl_2 (38.9 mmol) slowly at 0 °C. The resulting mixture was allowed to warm to 22 °C and stirred for 12 h. The mixture was then cooled to 0 °C, and the reaction was quenched by the slow addition of 50 mL water. Aqueous extraction with CH_2Cl_2 (3 × 50 mL), followed by drying of the organic layers over $MgSO_4$ and removal of the solvents in vacuo to afford an off-white solid, which was washed with hexanes, filtered, and dried in vacuo to afford 3.76 g of a white powder (5.44 mmol, 97% yield). Crystals of (*R*)-3,3′-bis(2,4,6-triisopropylphenyl)-2,2′-dihydroxy-1,1′-dinaphthyl (**23**) were obtained through slow evaporation of solvent from a CH_2Cl_2 solution. ^{1}H NMR (500 MHz, $CDCl_3$): δ 7.85 (d, J = 8.0 Hz, 2H, Ar*H*), 7.75 (s, 2H, Ar*H*), 7.36 (t, J = 8.0 Hz, 2H, Ar*H*), 7.32−7.26 (m, 4H, Ar*H*), 7.12 (s, 2H, Ar*H*), 7.10 (s, 2H, Ar*H*), 4.90 (s, 2H, O*H*), 2.95−2.93 (m, 2H, C*H*(CH$_3$)$_2$), 2.85−2.81 (m, 2H, C*H*(CH$_3$)$_2$), 2.69−2.65 (m, 2H, C*H*(CH$_3$)$_2$), 1.29 (d, J = 7.0 Hz, 12H, CH(C*H*$_3$)$_2$), 1.18 (d, J = 6.5 Hz, 6H, CH(C*H*$_3$)$_2$), 1.10−1.06 (m, 12H, CH(C*H*$_3$)$_2$), 1.01 (d, J = 6.5 Hz, 6H, CH(C*H*$_3$)$_2$). ^{13}C NMR (125 MHz, $CDCl_3$): δ 150.9, 149.4, 148.1, 148.0, 133.7, 131.0, 130.7, 129.4, 129.3, 128.5, 126.9, 124.8, 124.1, 121.5, 121.5, 113.4, 34.7, 31.2, 31.2, 24.6, 24.6, 24.4, 24.3, 24.2, 24.0. HRMS (FAB): calcd for $C_{50}H_{58}O_2$ 690.4437, found (M$^+$) 690.4435. Anal. Calcd for $C_{50}H_{58}O_2$: C, 86.91; H, 8.46. Found: C, 87.05; H, 8.72. $[\alpha]_{589}$ = 88.0 (c = 3.0, THF).

(*R*)-(+)-Mo(*N*-2,6-*i*-$Pr_2C_6H_3$)(CHCMe$_2$Ph)(3,3′-bis(2,4,6-triisopropylphenyl)-2,2′-dihydroxy-1,1′-dinaphthyl)(Py) (25). Complex (*R*)-(+)-Mo(*N*-2,6-*i*-$Pr_2C_6H_3$)(CHCMe$_2$Ph)(3,3′-bis(2,4,6-triisopropylphenyl)-2,2′-dihydroxy-1,1′-dinaphthyl)(THF) **(2a)** (0.5 g, 0.4 mmol) was dissolved in toluene (5 mL), and 0.5 mL pyridine (6.1 mmol) was added to this solution. The mixture was allowed to stir at 22 °C for 1 h. At this point, solvent was removed in vacuo, and the resulting yellow solid (**25**) was recrystallized from Et_2O. The single crystal was formed after 2 days at −30 °C. ^{1}H NMR (500 MHz, C_6D_6): δ 14.37 (s, *anti*-C*H*CMe$_2$Ph), 14.29 (s, *anti*-C*H*CMe$_2$Ph), 13.11 (s, 90% of 1H, *syn*-C*H*CMe$_2$Ph), 8.53 (d, J = 5.0 Hz, 90% of 1H, *syn*-Ar*H*), 8.09 (d, J = 5.0 Hz, 10% of 1H, *anti*-Ar*H*), 7.88−7.87 (m, 2H, Ar*H*), 7.78−7.65 (m, 2H, Ar*H*), 7.55, (s, 1H, Ar*H*), 7.53−7.47 (m, 1H, Ar*H*), 7.39 (d, J = 8.5 Hz, 2H, Ar*H*), 7.32−7.31 (m, 1H, Ar*H*), 7.23 (d, J = 1.5 Hz, 1H, Ar*H*), 7.15−6.90 (m, 8H, Ar*H*), 6.82−6.72 (m, 4H, Ar*H*), 6.66 (t, J = 6.0 Hz, 1H, Ar*H*), 6.54 (t, J = 7.5 Hz, 1H, Ar*H*), 6.04 (t, J = 7.0 Hz, 90% of 2H, *syn*-Ar*H*), 5.91 (t, J = 7.0 Hz, 90% of 2H, *anti*-Ar*H*), 3.98−3.94 (m, 90% of 1H, *anti*-Me$_2$C*H*), 4.12−4.07 (m, 10% of 1H, *anti*-Me$_2$C*H*), 3.78−3.72 (m, 10% of 1H, *anti*-Me$_2$C*H*), 3.61−3.57 (m, 10% of 1H, *anti*-Me$_2$C*H*), 3.48−3.43 (m, 90% of 1H, *anti*-Me$_2$C*H*), 3.28−3.18 (m, 2H, Me$_2$C*H*), 3.12−3.07 (m, 90% of 1H, *syn*-Me$_2$C*H*), 2.98−2.91 (m, 90% of 1H, *syn*-Me$_2$C*H*), 2.88−2.82 (m, 10% of 1H, *anti*-Me$_2$C*H*), 2.80−2.76 (m, 10% of 1H, *anti*-Me$_2$C*H*),

2.70−2.65 (m, 90% of 1H, *syn*-Me_2CH), 2.59−2.54 (m, 90% of 1H, *syn*-Me_2CH), 2.50−2.45 (m, 10% of 1H, *anti*-Me_2CH), 1.76 (s, 3H, $CHC(CH_3)_2Ph$), 1.45−0.63 (m, 45H, $CH(CH_3)_2$ and $CHC(CH_3)_2Ph$), 0.45 (d, $J = 7.0$ Hz, 6H, $(CH_3)_2CH$). ^{13}C NMR (125 MHz, C_6D_6): δ 309.4, 167.3, 166.1, 165.7, 161.9, 161.3, 160.8, 154.6, 153.5, 152.1, 151.7, 151.6, 150.7, 149.9, 148.8, 148.5, 148.4, 148.2, 148.0, 147.6, 147.6, 147.5, 147.5, 147.4, 147.3, 147.2, 147.1, 147.0, 146.2, 143.7, 141.0, 138.5, 138.4, 138.2, 137.3, 137.2, 137.0, 136.9, 136.9, 136.8, 136.1, 135.9, 135.5, 133.6, 133.3, 133.0, 132.7, 132.0, 131.3, 131.2, 130.9, 130.4, 130.3, 130.1, 130.0, 129.7, 129.6, 129.0, 128.9, 128.8, 128.7, 128.0, 127.7, 127.5, 127.2, 127.1, 127.0, 126.8, 126.7, 126.5, 126.4, 126.2, 125.9, 125.9, 125.8, 125.7, 124.2, 124.1, 123.8, 123.7, 123.6, 123.4, 123.3, 123.2, 123.2, 123.1, 122.9, 122.8, 121.6, 121.4, 121.3, 121.3, 121.1, 121.1, 120.9, 120.8, 120.7, 120.6, 120.6, 120.5, 66.3, 54.3, 53.6, 52.8, 35.4, 35.2, 35.0, 34.8, 34.6, 32.8, 32.3, 32.2, 32.1, 31.8, 31.7, 31.4, 31.3, 31.2, 31.1, 31.0, 30.8, 30.6, 29.9, 29.6, 29.5, 29.2, 28.6, 28.2, 27.8, 27.5, 27.4, 27.0, 26.6, 26.5, 26.4, 26.2, 25.9, 25.8, 25.7, 25.6, 25.6, 25.4, 25.4, 25.3, 25.1, 25.1, 25.0, 24.9, 24.9, 24.8, 24.7, 24.7, 24.7. Anal. Calcd for $C_{77}H_{90}N_2O_2Mo$: C, 78.94; H, 7.74; N, 2.39. Found: C, 79.06; H, 7.79; N, 2.29.

Acknowledgment. This work was supported by the NIH (GM-47480 to A.H.H.), the NSF (CHE-9905806 to A.H.H. and CHE-9700736 to R.R.S.), the American Chemical Society (graduate fellowship in organic chemistry to D.S.L., sponsored by Boehringer-Ingelheim), and the Natural Sciences and Engineering Research Council of Canada (predoctoral fellowship to J.Y.J.). We thank J. B. Alexander for experimental assistance and helpful discussions.

Supporting Information Available: Spectral and analytical data for recovered starting materials and reaction products. Tables of crystallographic experimental details, atomic coordinates and isotropic displacement parameters, interatomic bond lengths and angles, anisotropic displacement parameters, and hydrogen coordinates for Mo complex **25**. This material is available free of charge via the Internet at http://pubs.acs.org.

JA991432G